Characterization and Design of Magnetic Coils for the Magneto-Inertial Fusion Electrical Discharge System (MIFEDS)

Felix Q. Jin

Brighton High School
Rochester, NY

Advisor: Dr. Gennady Fiksel

Laboratory for Laser Energetics
University of Rochester
Rochester, NY
November 2011

Abstract

The Magneto-Inertial Fusion Electrical Discharge System (MIFEDS) is used to provide a strong pulse of magnetic field required for a broad range of nuclear fusion and astrophysical applications. A dual-coil system currently used for MIFEDS was characterized, and a better single-coil design was developed. First, a mathematical formula was derived, and the dynamics of the coil resistive heating, including the current skin effect and temperature diffusion, was calculated. The results show that the coil heating is small. Second, a diagnostic method using a quadratic approximation of current waveform peaks was developed, which can determine when coil arcing occurs based on frequency analysis of the coil current waveform. Third, two computer programs were written to calculate and map the magnetic field and the coil inductance, respectively. Results from these theoretical calculations indicate that the existing dual-coil design for MIFEDS could be improved and a single-coil design could provide a stronger and more uniform field. A single coil based on this new design was fabricated and experimentally tested, and results reveal that the magnetic field generated by the single coil is much stronger than that of the dual-coil design. This will result in better energy confinement for laser inertial fusion and thus higher fusion efficiency.

1. Introduction

Nuclear fusion energy is the energy generated through nuclear fusion processes, in which two light atomic nuclei fuse together to form a heavier nucleus. Unlike energy generated by fossil fuel and nuclear fission power, nuclear fusion is sustainable and environmentally clean. However, nuclear fusion energy remains under research and development stages in the United States and other countries. The Laboratory for Laser Energetics at the University of Rochester is one such facility that focuses on nuclear fusion studies, specifically inertial confinement fusion, which uses the 60-beam OMEGA laser system to initiate fusion by heating and compressing a cryogenic target.

The Magneto-Inertial Fusion Electrical Discharge System (MIFEDS) is used to provide a strong pulse of magnetic field required for magneto-inertial fusion (MIF) and for other applications such as astrophysics and high-energy-density plasmas.[1] MIFEDS uses strong magnetic fields to confine fusion fuel while the fuel is heated into a plasma. A strong magnetic field confines the plasma and reduces thermal loss. In MIF, magnetic fields are used to slow down plasma losses, and inertial compression is used to heat the plasma. One of the challenges for MIF is the need to form high-strength magnetic fields at the focus of the reaction. MIFEDS can be flexibly added to the OMEGA Laser System when MIF or other experiments involving strong magnetic fields are planned. Currently a dual magnetic coil design is used in MIFEDS to generate magnetic fields for high-energy-density plasma studies with the OMEGA Laser System at the University of Rochester. However, the physical characteristics of this dual magnetic coil device have not been fully investigated.

In this work, a mathematical formula, a diagnostic method and two computer programs were developed and used to determine the dynamics of the coil resistive heating, the time of coil

arcing, the strength of the magnetic field, and the coil inductance. Results from these theoretical calculations indicate that the current dual-coil design for MIFEDS could be improved by using a single-coil design. Furthermore, a single-coil device was fabricated and experimentally tested, and results reveal that the magnetic field generated by a single coil is much stronger and more uniform than that of the dual-coil design.

2 Mathematic Models and Experimental Methods

2.1 *The MIFEDS device*

MIFEDS is a system which produces a strong magnetic field in the target zone. A pulse of electric current travels through a coil at the end of the transmission line to produce this magnetic field. High-voltage (HV) capacitors are used to store the energy before firing, and a laser trigger beam is aimed at a spark gap. When the laser fires, it initiates the electrical discharge, which dumps the current through the transmission line and coil before returning through the reverse side of the transmission line. The other end of the transmission line is reconnected with the HV capacitors. MIFEDS is inserted into the OMEGA target chamber through one of the Ten-Inch Manipulator (TIM) ports.

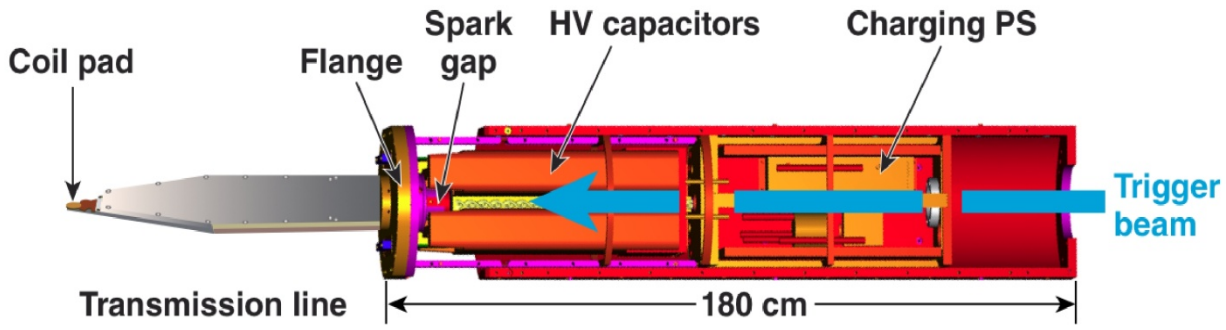

Fig. 1. Diagram of the MIFEDS assembly
High-voltage capacitors are charged, and then discharged by a spark gap, which is triggered by a laser trigger. Current travels down the transmission line and through the coils, generating a high magnetic field.

The MIFEDS system behaves like an LRC circuit with most of the capacitance being part of the HV capacitors and most of the inductance part of the coil and transmission line. The natural frequency depends on the exact coil that is used. However, in general, the initial period of the current is about 600 ns and the discharge current peaks at around 40 kA. The coil itself is fabricated out of high-purity sheet copper and insulated with kapton. The transmission line is composed of two parallel plates of aluminum also insulated with kapton.

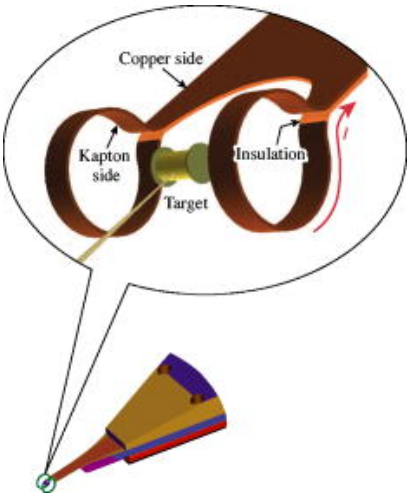

Fig. 2. Diagram of MIFEDS coil
As current flows through the coils, a strong magnetic field is created in the area around the target.[2]

2.2 The magnetic field-measuring apparatus

A Faraday rotation setup was used to measure the strength of the magnetic fields produced by MIFEDS. A Faraday probe was placed in between the two coils, and polarized light from a dedicated probe laser was passed through the probe. The probe's crystal rotates the polarization of light in proportion to the external magnetic field due to the Faraday effect. By measuring the amount of rotation, the magnetic field strength can be determined. The rotation angle θ is given by the expression $\theta = Blk$, where B is the magnetic field strength parallel to the light, l is the length of the crystal, and k is the Verdet constant of the crystal, which for our probe was 100 rad/T m. The test chamber and magnetic field-measuring apparatus are shown in Fig. 3.

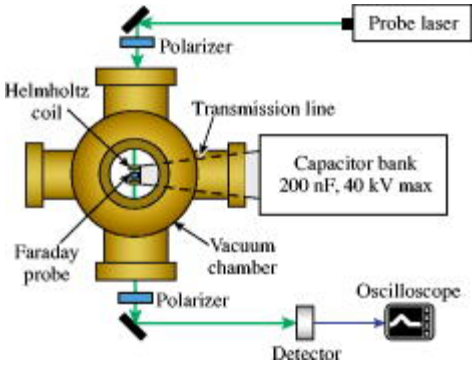

Fig. 3. Diagram of the magnetic field-measuring apparatus
A Faraday rotator was used inside the testing chamber to determine the magnetic field strength.[2]

The light intensity is measured by a detector and the data is collected with an oscilloscope. The field is then determined using Eq. (1) and Malus's law,

$$I = I_0 \cos^2 \theta \tag{1}$$

which gives the detected light intensity I as a function of the angle of rotation θ and the initial full intensity I_0. The second polarizer is configured so that without a magnetic field, the measured angle would be $\pi/2$ radians as this allows for maximum sensitivity in both field directions.

The current going through the system can also be measured and analyzed. This is done through a Rogowski pickup coil, a device which measures high-speed electrical current pulses. This coil is placed around the internal portion of the transmission line, near the HV capacitors.

2.3 Temperature of magnetic coils

The temperature of the MIFEDS magnetic coils was of importance because previous experiments and calculations suggested that some copper may be evaporating during discharge.[2] An equation was developed to model the temperature of the coils, taking into account skin effect current, temperature-dependant resistance, and resistive heating. The first, basic model considered only resistive heating and treated current density as uniform. According to Joule's law, the power P of resistive heating of the circuit is equal to the rate of energy transferred as heat to the coil. This primary expression is

$$P = \frac{dW}{dt} = I^2 R = C \frac{dT}{dt} \tag{2}$$

where I is the current, R is the resistance, C is the heat capacity of the material, and T is the temperature. The current becomes a function of time since the circuit is an oscillator, and the resistance becomes a function of the temperature of the coil.

Heat-dependent resistance follows the equation $R(T) = R_0[1 + \alpha(T - T_0)]$, where α is the temperature coefficient of resistance for copper, and R_0 is the initial resistance at some temperature T_0.

The skin effect current creates a non-uniform current distribution within the coil, and the current is mostly concentrated close to the outside of the coil. In order to determine a maximum bound for temperature, only the surface of the coil was considered, and radiative cooling was ignored. For an infinitely thick slab where x=0 is the surface and where the slab extends in the positive x-direction, skin effect calculations for the surface yield the following equations:

$$\delta = \sqrt{\frac{2}{\omega\mu\sigma}} \tag{3}$$

$$\frac{\partial j}{\partial x} = \frac{\mu_0\sigma}{P}\frac{\partial I}{\partial t} \tag{4}$$

$$j(x,t) = j_0 e^{-x/\delta} e^{i(\omega t - x/\delta)} \tag{5}$$

where δ is the skin depth, ω is the frequency, μ is the magnetic permeability of copper, μ_0 is the vacuum permeability, σ is the electrical conductivity, I is the total current entering the system, j is the current density, and j_0 is the maximum current density which occurs at the surface. Solving equations 3, 4, and 5 gives

$$j(x,t) = \frac{I_0}{\delta P} e^{-x/\delta} e^{i(\omega t - x/\delta)}, \tag{6}$$

which, at the surface (x=0), simplifies to

$$j(0,t) = \frac{\sqrt{2}I_0}{\delta P}\sin(\omega t + \frac{\pi}{4}). \tag{7}$$

Thus, the maximum current density at the surface of the coil is $\frac{\sqrt{2}I_0}{\delta P}$. Since the model sets t=0 when MIFEDS first fires, the current waveform at the surface can be approximated by

$$I(t) = \frac{\sqrt{2}I_0}{\delta P}\sin \omega t. \tag{8}$$

The heat capacity C is equal to the mass times the specific heat c. The final equation should evaluate current density instead of current, so the expression is divided by ρ, the density of copper. The final differential equation for temperature is

$$\frac{dT}{dt} = \frac{j^2(t)R(T)}{C\rho} = \frac{2I_0^2 \sin^2(\omega t)R_0[1 + \alpha(T - T_0)]}{\delta^2 P^2 C\rho}. \tag{9}$$

2.4 Frequency measurement and arcing analysis

Because the MIFEDS circuit is connected in a loop, it behaves like an LRC circuit. The natural frequency is inversely proportional to the square root of the inductance and the capacitance. This frequency can be determined from magnetic field or current measurements. In some tests, the magnetic field only oscillates for one period before collapsing. An increase in frequency is also observed after the field collapses, which indicates that arcing occurred because the inductance of the arc is much lower than that of the coil. Due to a phenomenon not yet fully explored, the first period of magnetic field is much weaker when there is an arc. Ensuring that arcing does not occur too soon allows it to be confirmed that a magnetic field is generated. A quadratic-regression method was used to estimate the peaks of the current waveform and determine the period. When the period drops, arcing is predicted to have happened.

2.5 Magnetic field mapping

The magnetic field generated by MIFEDS was of interest to examine field properties and to determine the location and strength of the maximum field produced. The general equation for the magnetic field generated by a current is given by the Biot-Savart law:

$$\vec{B} = \int \overrightarrow{dB} = \int \frac{\mu_0}{4\pi}\frac{I\overrightarrow{dl} \times \vec{s}}{|s|^3}. \tag{10}$$

Two parallel circular loops of coil were used as an approximation for the actual case. Fig. 4 is a sketch of the geometry and the variables used in the following derivation. A cross sectional contour diagram of the field sliced through the center was desired, so the point of interest was fixed in the yz-plane, with its x-coordinate equal to 0.

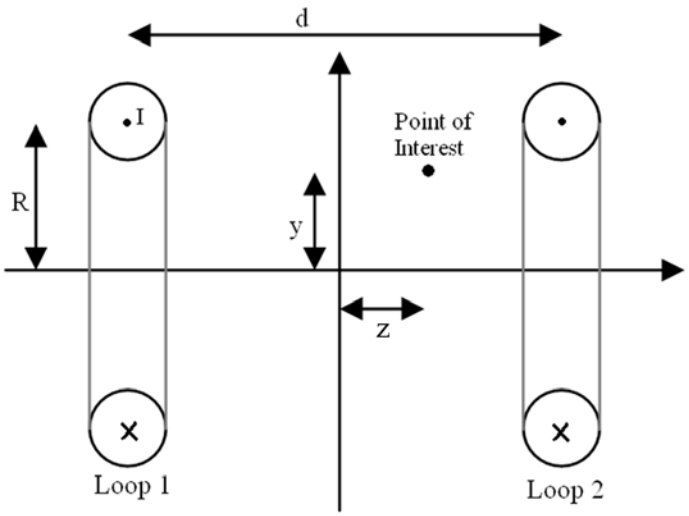

Fig. 4a. Cross-section of dual MIFEDS coils
This diagram shows the names of the variables assigned to the various properties of the coil configuration. The **i**(x) direction is into the page, **j**(y) direction is to the top, and **k**(z) direction is to the right.

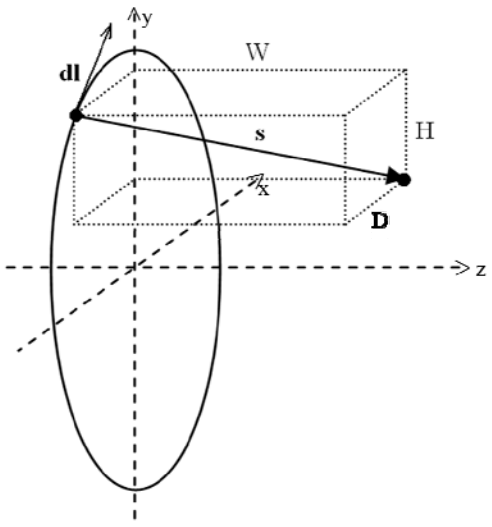

Fig. 4b. Diagram of single loop
The integral is evaluated along the path of the current (the circle), and **s** is the vector from the circle to the point of interest.

The variables D (depth), H (height), and W (width) are the components of the s-vector from the loop to the point of interest such that $\vec{s} = D\hat{\imath} + H\hat{\jmath} + W\hat{k}$. The D variable corresponds with the x-axis, H corresponds with the y-axis, and W corresponds with the z-axis. The magnitude of **s** is therefore $\sqrt{D^2 + H^2 + W^2}$. The integration starts from the top of the loop and goes around so that $\overrightarrow{dl} = dl\cos\theta\,\hat{\imath} - dl\sin\theta\,\hat{\jmath}$, where θ is the angle around the loop starting at the top. The cross product is $\overrightarrow{dl} \times \vec{s} = -Wdl\sin\theta\,\hat{\imath} - Wdl\cos\theta\,\hat{\jmath} + (H\cos\theta + D\sin\theta)dl\,\hat{k}$.

Analysis of the geometry yields the equations, $D = R\sin\theta$ and $H = R\cos\theta - y$, where y is the **j**-component of the distance from the center of the circle to the point (see Fig. 4a). The

identity $\theta = l/R$ is used to convert from the angle around the circle to the circumference traveled.

The equation for the magnetic field at a point (0, y, z) for a coil centered at the origin is

$$\vec{B} = \frac{\mu_0 I}{4\pi}\int_0^{2\pi} \frac{-z\sin\frac{l}{r}\hat{\imath} - z\cos\frac{l}{r}\hat{\jmath} + R\,\hat{k}}{\left[\left(R\sin\frac{l}{r}\right)^2 + \left(R\sin\frac{l}{r} - y\right)^2 + z^2\right]^{3/2}} dl. \tag{11}$$

To model two coils, the initial current I_0 is divided by 2, and an additional term is added. The W variable for the first coil is z-d/2 and for the second coil is z+d/2, where d is the distance between the two coils:

$$\vec{B} = \frac{\mu_0 I}{4\pi}\int_0^{2\pi} \left(\frac{-(z-\frac{d}{2})\sin\frac{l}{r}\hat{\imath} - (z-\frac{d}{2})\cos\frac{l}{r}\hat{\jmath} + R\,\hat{k}}{\left[\left(R\sin\frac{l}{r}\right)^2 + \left(R\sin\frac{l}{r} - y\right)^2 + (z-\frac{d}{2})^2\right]^{3/2}} \right. \tag{12}$$

$$\left. + \frac{-(z+\frac{d}{2})\sin\frac{l}{r}\hat{\imath} - (z+\frac{d}{2})\cos\frac{l}{r}\hat{\jmath} + R\,\hat{k}}{\left[\left(R\sin\frac{l}{r}\right)^2 + \left(R\sin\frac{l}{r} - y\right)^2 + (z+\frac{d}{2})^2\right]^{3/2}} \right) dl.$$

2.6 A new coil design

Initial calculations from the development of the magnetic field mapping suggested that a single magnetic coil could produce a stronger magnetic field than the dual-coil design that was used. However, a single coil does have a much higher impedance. In order to reduce this, a flatter coil was suggested because it would have similar impedance to that of the dual-coil design while possibly providing a stronger and more uniform magnetic field. To model a flat coil, multiple terms were added to the equation, with the

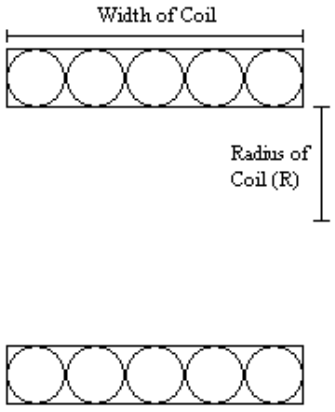

Fig. 5. Cross section showing how a flat single-coil was modeled
Circular coils stacked on each other approximate the flat coil.

loops being adjacent to each other. Using magnetic field mapping and calculations of inductance and impedance, it was determined that a coil 3 millimeters in width would be ideal.

3 Results

3.1 Solving for temperature

To solve the coil-temperature differential equation, a fourth-order Runge-Kutta-method program was written in MATLAB. The differential equation the program used was the previously derived Eq. 9. The average amplitude of the first period is 40 kA, so a value of 20 kA was used to model one of the two coils.

To approximate the perimeter of a cross section of the coil, a thickness of 0.25 mm and a width of 1 mm were used. The heat capacity C was calculated by multiplying the specific heat of copper by the mass per unit length, which was determined using the cross-sectional area and the density of copper.

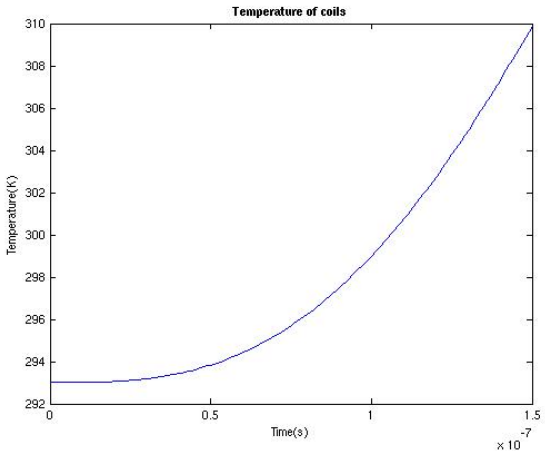

Fig. 6. Plot of the predicted temperature of MIFEDS coil during the first 150 ms
The initial temperature was set to room temperature. The coil theoretically sees an increase in temperature of about 17 Kelvin.

MIFEDS is fired 150 milliseconds before the laser shot because the peak of the magnetic field strength occurs 150 ms after the initial discharge. Fig. 6 shows the plot generated by the program. Based on these results, it was determined that the coil heating was minimal, and the copper was not evaporating before the laser shot.

3.2 Analysis of Arcing

Current data collected from the Rogowski coil in MIFEDS (Fig. 7a) was used for analysis. The data for the peaks of the current were then isolated. The peak of the quadratic regression for the data was used to approximate the actual peak. Fig. 7b shows one such analysis in which arcing clearly occurred. However, it was late enough to not have affected the magnetic field

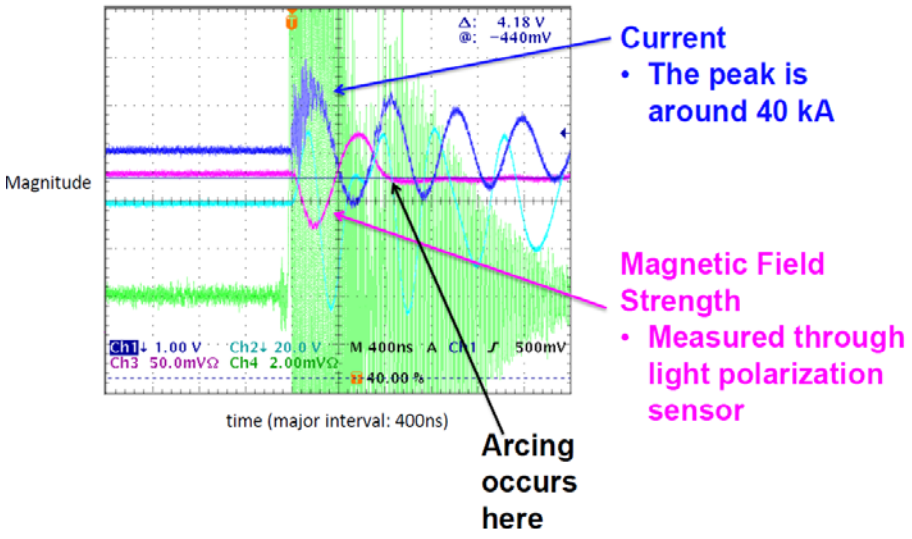

Fig. 7a. Data from the oscilloscope demonstrating arcing When arcing occurs, there is a slight change in frequency, and the magnetic field is no longer produced. The green and teal lines are from two other diagnostic tools not used for this experiment.

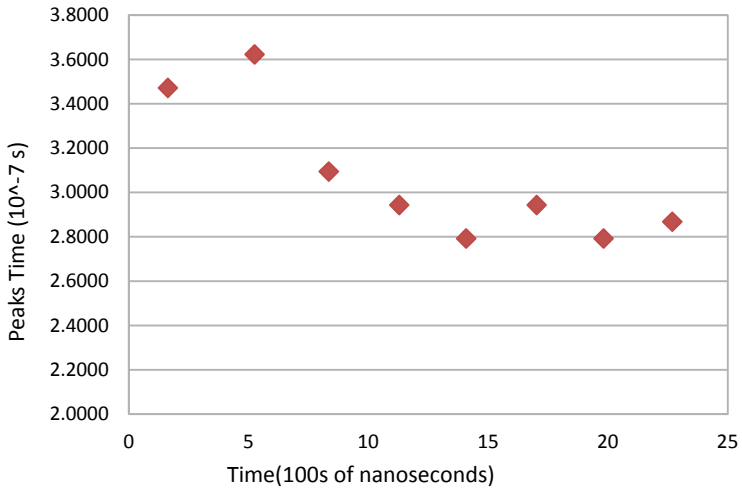

Fig. 7b. Analysis of the period of the waveform At the second period, arcing occurs, indicated by the drop in the period.

strength of the first half-period, which is when the laser would fire. On August 3 2011, an astrophysics experiment was conducted with the OMEGA laser and MIFEDS to study the effect of strong magnetic fields on certain particles. As shown in Fig. 8 frequency analysis was used to

confirm that the magnetic field did not collapse too early. Results indicated that the magnetic field was most likely stable, but may have been weaker in a few cases due to the arcing effect.

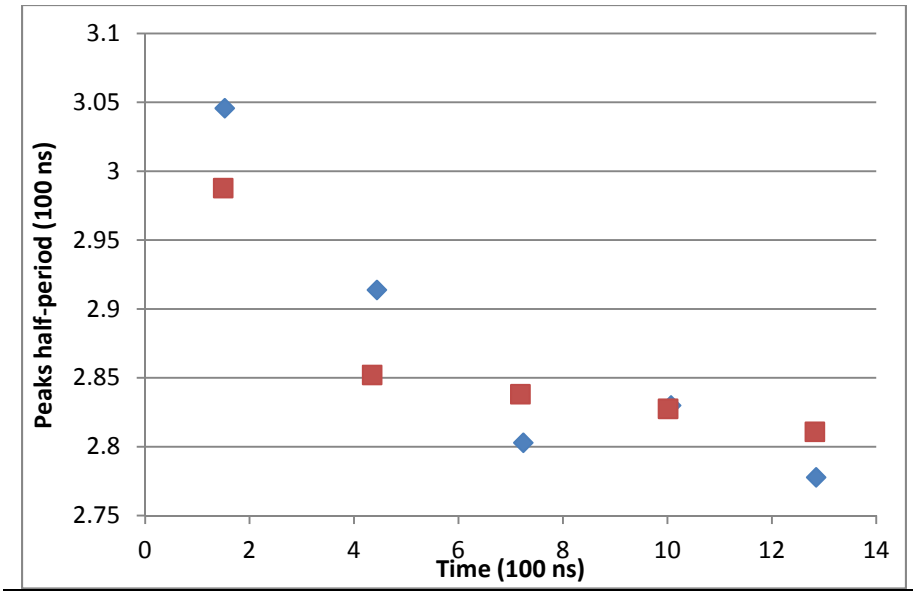

Fig. 8. Frequency analysis results from the 8-03-11 experiment
Arcing most likely occurred after the first half-period. This may have reduced the magnetic field strength during the shot.

3.3 Magnetic field maps

Code written in MATHEMATICA was used to numerically integrate equations (11) and (12) for the magnetic field and to create the contour plots. For the dual-coil map, a radius of 6 mm and a separation between the coils of 13 mm was used. Fig. 9 represents the result of these calculations. These results show that most of the magnetic field is concentrated at the center of each coil instead of between the coils. Additionally, the field is only uniform at the center, not near the edges.

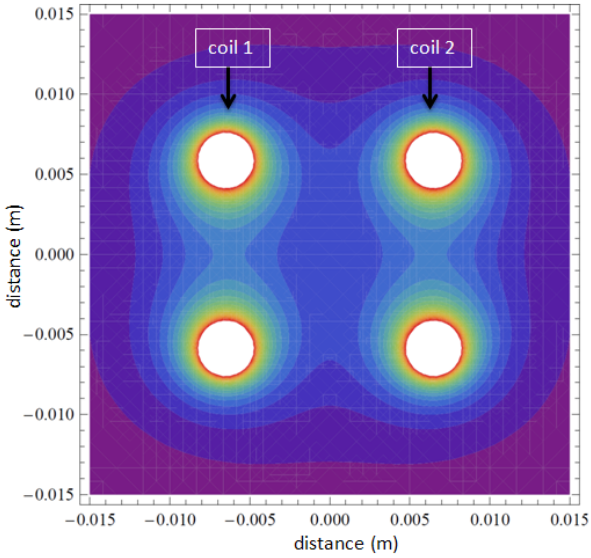

Fig. 9. Magnetic field contour plot for the standard dual-coil design
The outermost area represents a field strength of 0 to 0.5 T and the contour interval is 0.5 T.

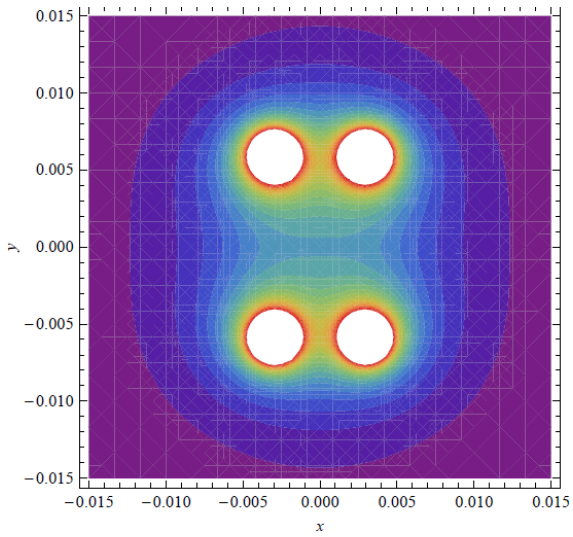

Fig. 10. Magnetic field contour plot for a Helmholtz coil
A Helmholtz arrangement produces the smoothest field at the center and in between the coils.

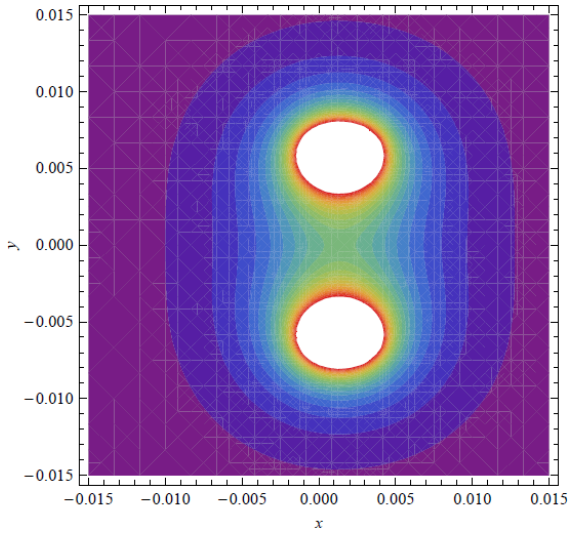

Fig. 11. Magnetic field contour plot for a flat single coil
The single coil design generates a much stronger and concentrated magnetic field at the center.

A Helmholtz coil arrangement is one where there are two coils and the distance between them is half the radius of a coil. As shown in Fig. 10, a Helmholtz coil produces the most uniform field at the center. A flat single-coil design was suggested to produce stronger and more uniform magnetic fields than the dual-coil design. Results (Fig. 11) indicate that the magnetic field for a single flat coil is much stronger than for a dual coil. Although the field is not extremely smooth, the single-coil field is closer to the Helmholtz field than is the field of the dual-coil design that was originally used (Fig. 9).

3.4 Experimental testing of the new coil design

A MIFEDS coil consisting of a single loop with a width of 3 mm was cut and bent out of a 0.25 mm-thick copper stock. Because of certain limitations of the viewing geometry, the Faraday probe could not be placed at the center of the loop. Instead, the probe was placed to the side of the coil, and the measurement at the edge would be converted to a value for the magnetic

field at the center. The new coil was placed into the test chamber, and MIFEDS was charged and fired. Fig. 12a shows the data collected from the oscilloscope for this test. The dark blue line is current, and the purple line is magnetic field strength. Although arcing occurred quickly since the magnetic field stopped oscillating after the peak, the field was still strong.

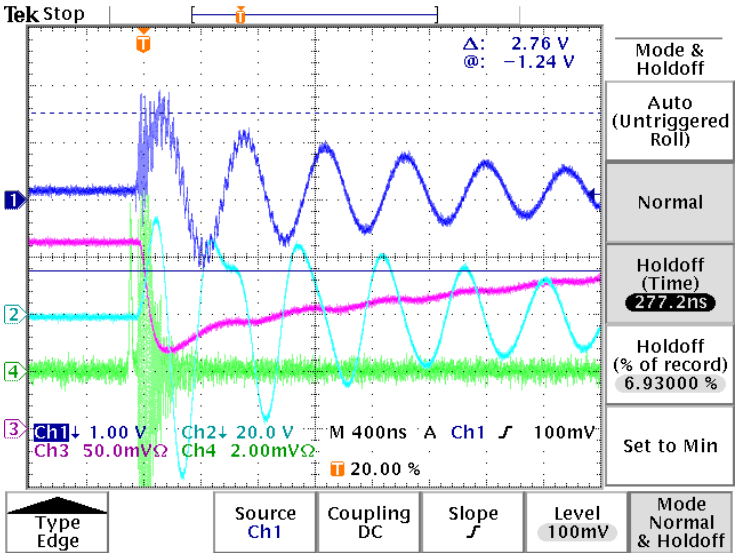

Fig. 12a. Current and magnetic field data for flat coil test
Arcing occurs very early on in this test, but the single flat coil produced a much stronger field.

Fig. 12b. Image of the Faraday probe location
This picture was used to determine the distance from the probe to the center. Coil width is 3 mm

The measured magnetic field strength was 3.15 T, which is the strength at the location of the probe, placed besides the coil. The image shown in Fig. 12b was used to find how far the probe was from the center. Using calculations from the magnetic field maps, a conversion ratio was determined to find the field strength at the center. The probe was about 1.5 mm from the center, so the maximum field strength at the center was predicted to be 4.37 T, much stronger than the dual-coil design, which produced a field strength averaging about 1.6 T.

4 Conclusions

Calculations and mathematical models were produced to characterize the magnetic coils used for the MIFEDS. A model of coil heating was produced, which predicted that the coils were not evaporating. Frequency-analysis methods were used to predict coil arcing and to confirm the successful generation of a magnetic field for experiments involving MIFEDS. The magnetic field produced by the coil was analyzed and mapped. Based on these results, a new single-coil design was proposed, fabricated, and experimentally tested; the results of the test confirmed that this design produced stronger magnetic fields.

Future research will improve upon both the temperature and magnetic field models. The goal is to produce new designs and modifications to MIFEDS that will improve efficiency, field strength, and field uniformity. These improvements and the increased productivity will ultimately allow MIFEDS to meet the requirements of and be used in more experiments and applications requiring strong magnetic fields.

Acknowledgements

I would like to thank Dr. Gennady Fiksel for being my research advisor and helping me with the project, Po-Yu Chang for his teaching and technical assistance, the program director Dr. R. S. Craxton for providing me this research opportunity, and Dr. Anatoly Spitkovsky at the Department of Astrophysics, Princeton University for providing me the opportunity to work with him and help conduct a laser shot experiment at the Laboratory for Laser Energetics, University of Rochester.

References

[1] Gotchev *et al*., "Laser-Driven Magnetic-Flux Compression in High-Energy-Density Plasmas, *Physical Review Letters,* **103**:215004, 2009.

[2] Gotchev *et al*., "Seeding magnetic fields for laser-driven flux compression in high-energy-density plasmas," *Review of Scientific Instruments*, **80**:043504, 2009.